

# Soil internal forces contribute more than raindrop impact force to rainfall splash erosion

Feinan Hu<sup>a,b</sup>, Jingfang Liu<sup>c,a</sup>, Chenyang Xu<sup>c</sup>, Wei Du<sup>c</sup>, Zhihua Yang<sup>b</sup>, Xinmin Liu<sup>d</sup>, Gang Liu<sup>a,b,\*</sup>, Shiwei Zhao<sup>a,b,c</sup>

<sup>a</sup> State Key Laboratory of Soil Erosion and Dryland Farming on the Loess Plateau, Institute of Soil and Water Conservation, Northwest A&F University, Yangling, Shaanxi 712100, China

<sup>b</sup> Institute of Soil and Water Conservation, Chinese Academy of Sciences and Ministry of Water Resources, Yangling, Shaanxi 712100, China

<sup>c</sup> College of Resources and Environment, Northwest A&F University, Yangling, Shaanxi 712100, China

<sup>d</sup> Chongqing Key Laboratory of Soil Multi-Scale Interfacial Process, College of Resources and Environment, Southwest University, Chongqing 400715, China

## ARTICLE INFO

Handling Editor: Morgan Cristine L.S.

### Keywords:

Electrostatic force  
Hydration force  
Raindrop impact force  
Rainfall kinetic energy

## ABSTRACT

Soil internal forces, including electrostatic, hydration and van der Waals, play critical roles in aggregate stability, erosion, and other processes related to soil and water. However, the extent to which soil internal forces influence splash erosion during rainfall remains unclear. In the present study, we used cationic-saturated soil samples to quantitatively separate the effects of soil internal and raindrop impact forces (external) on splash erosion through simulated rainfall experiments. An electrolyte solution was employed as rainfall material to represent the combined effects of soil internal and external forces on splash erosion. Ethanol was used to simulate the sole effect of soil external force on splash erosion. The soil splash erosion rate increased with increasing rainfall kinetic energy in experiments with electrolyte solution and ethanol and was also greatly influenced by soil internal forces. Moreover, the soil splash erosion rate increased first (from 1 to  $10^{-2}$  mol L<sup>-1</sup>) then leveled off (from  $10^{-2}$  to  $10^{-4}$  mol L<sup>-1</sup>) with decreasing electrolyte concentration in the bulk solution. This finding was in agreement with the theoretical analysis of soil internal forces. The contribution rate of soil internal forces on splash erosion was > 65% at a low electrolyte concentration (<  $10^{-2}$  mol L<sup>-1</sup>) and only 3%–25% at an electrolyte concentration of 1 mol L<sup>-1</sup>. Even though the electrolyte concentration of the soil bulk solution reached  $10^{-1}$  mol L<sup>-1</sup>, the contribution rate of soil internal forces to splash erosion was > 50%. Hence, soil internal forces exerted higher contribution to rainfall splash erosion than raindrop impact force under most field conditions. This work provides new understanding of the mechanism of soil splash erosion and establishes the possibility of controlling splash erosion by jointly regulating the soil internal and external forces.

## 1. Introduction

Splash erosion mainly caused by raindrop impact is an important process and the first step of soil erosion during rainfall (Legout et al., 2005a, 2005b; Vaezi et al., 2017; Fernández-Raga et al., 2017). Splash erosion has two main direct consequences, namely, breakdown of top soil aggregates and movement of finer soil particles (Legout et al., 2005a; Warrington et al., 2009; Angulo-Martínez et al., 2012), which may lead to surface sealing, decrease in soil porosity, increase in runoff and sediment, and negatively influence on the sustainable development of agriculture and ecological environment (Le Bissonnais, 1996; Uri, 2000; Falson et al., 2012; Vaezi and Bahrami, 2014; Mekonnen et al., 2015; Parras-Alcántara et al., 2016; Zhang et al., 2017; Yaghibi et al., 2018). Therefore, an effective method must be developed to protect

aggregates against the disruptive effects of raindrop impact, shear strength of flowing water, and freezing/thawing cycles.

Splash erosion starts with the disintegration of soil aggregates into small particles (Shainberg et al., 1992); in this regard, soil aggregate stability is often used as an indicator of soil erodibility (Barthès and Roose, 2002; Wuddivira et al., 2009; Ma et al., 2014; Xiao et al., 2017, 2018). The interaction of internal forces (electrostatic, hydration and van der Waals force) are crucial for initiation of the soil aggregate breakdown (Hu et al., 2015; Xu et al., 2015; Huang et al., 2016). Among these soil internal forces, electrostatic and hydration forces are repulsive and induce soil aggregate breakdown; meanwhile, van der Waals force is attractive and restrains aggregate dispersion (Huang et al., 2016). In general, as rainfall enters the soil, strong hydration and electrostatic forces between soil particles in the aggregates build up

\* Corresponding author at: No. 26, Xi'nong Road, Institute of Soil and Water Conservation, Northwest A&F University, Yangling, Shaanxi 712100, China.  
E-mail address: [gliu@foxmail.com](mailto:gliu@foxmail.com) (G. Liu).

rapidly with decreasing electrolyte concentration in the soil bulk solution; this phenomenon leads to the breakdown of aggregates and the immediate release of micro-aggregates/finer particles (Hu et al., 2015). Theoretically, soil internal forces could reach as high as hundreds of thousands of atmospheric pressure among soil particles (Li et al., 2013). The net pressure, i.e. the sum of electrostatic, hydration and van der Waals forces among soil particles, controls aggregate swelling, dispersion, or breakdown. Holthusen et al. (2010) measured the rheological parameters for soils with different salt concentrations; the results indicated that soil aggregate stability at the microscale increased with increasing potassium concentration in the soil solution due to the change in the soil particle interaction forces. Li et al. (2013) reported that the net pressure of soil internal forces among particles strengthened with decreasing electrolyte concentration in the bulk solution, resulting in increased soil particle transport during simulated rainfall. Yu et al. (2017) found that the removal of soil organic matter decreased the soil aggregate stability mainly due to the decreasing van der Waals force among soil particles. These studies indicate that soil internal forces could significantly affect aggregate stability and thus splash erosion during rainfall. In our recent study, through the simulated rainfall experiments, we demonstrated that splash erosion could be due to the coupling effects of soil internal and raindrop impact forces (Hu et al., 2018). During splash erosion, soil internal forces mainly induce aggregate breakdown and release of fine soil particles when the soil is wetted; this process supplies the original material for rainfall splash erosion.

Besides, raindrop impact force is the driving mechanism that causes soil particle movement (Le Bissonnais and Singer, 1993; Kinnell, 2005; Legout et al., 2005a; Oliveira et al., 2013). This type of force is regarded as the main external factor that affects splash erosion. If raindrop impact would be totally eliminated, then splash erosion will not occur during rainfall. Rainfall properties, such as shape and size, intensity, kinetic energy, and their various combinations, exert important effects on splash erosion (Jayawardena and Rezaur, 2000; Wei et al., 2007; Lu et al., 2008; Pieri et al., 2009; Ziadat and Taimeh, 2013; Fu et al., 2016). In any case, the most important parameter that influences splash erosion is raindrop kinetic energy (Fernández-Raga et al., 2010; Vaezi et al., 2017). In general, the splash erosion rate increases with increasing raindrop kinetic energy (Hu et al., 2016). Raindrop impact has two main consequences: breakdown of surface soil aggregates and movement of fine particles (Legout et al., 2005a, 2005b). But, unlike soil internal forces, raindrop impact force mainly influences the movement of fine particles (Hu et al., 2018).

Overall, rainfall splash erosion is affected by two erosive factors: soil internal and raindrop impact (or external) forces (Hu et al., 2018). Soil internal forces induce aggregate breakdown, which could supply certain amounts of fine soil fragments for splash erosion. Soil external forces, i.e., raindrop impact force, induce the movement of soil fragments (Legout et al., 2005a; Fernández-Raga et al., 2017). Hence, soil internal forces determine the “source” (the amount of fine soil particles released from macro-aggregates) of splash erosion; meanwhile, soil external force controls the movement of fine particles. Therefore, the coupling effect of soil internal and external forces could result in splash erosion. However, the extent to which soil internal forces influence splash erosion during rainfall remains unclear. Determining the contribution of soil internal forces to splash erosion will improve our knowledge on the nature of erosivity and its influencing factors. Results could also provide a basis for developing a more effective method for controlling the risk of soil erosion by jointly regulating the soil internal and external forces.

Thus, we hypothesize that soil internal forces have higher contribution to splash erosion rate during rainfall than raindrop impact force. In this study, electrolyte solution was used as rainfall material to represent the combined effects of soil internal and external forces on splash erosion. Ethanol was employed to simulate the sole effect of soil external force (raindrop impact) on splash erosion. This work aims to

quantitatively evaluate the effects of soil internal forces on splash erosion through simulated rainfall experiments.

## 2. Materials and methods

### 2.1. Materials

Soil samples were collected from Yangling (108°2'30"E, 34°18'14"N), Shaanxi Province, which is located in the south of the Loess Plateau in China. Soil erosion in this area is usually serious during the rain period (from July to September). The major crops planted in this region are winter wheat (*Triticum aestivum* Linn) and maize (*Zea mays* L.). The studied soil is Lou soil, which is classified as Calcic Cambisols (according to the FAO soil classification). Soils were sampled from the top 0–20 cm layer of three representative cultivated lands and mixed. X-ray diffraction analysis showed that the dominant clay minerals of the soil were illite, kaolinite, chlorite, and montmorillonite. The contents of clay, silt, and sand in the soils were 25.4%, 40.5%, and 34.1%, respectively, which were measured using a Malvern Mastersizer 2000 laser diffraction device (Malvern Instruments Ltd., UK). According to the combined method for determination of surface properties proposed by Li et al. (2011), the cation exchange capacity (CEC) and specific surface area (SSA) of the soil were 23.2 cmol<sub>c</sub> kg<sup>-1</sup> and 41.5 m<sup>2</sup> g<sup>-1</sup>, respectively. The pH and soil organic matter content were 8.01 and 6.1 g kg<sup>-1</sup>, which were measured using traditional methods (Sparks et al., 1996).

### 2.2. Soil sample treatments

Other factors should be kept as constant as possible for investigating the effects of soil internal forces on splash erosion. Thus, soil samples were first saturated with the given cation species. According to previous studies (Li et al., 2015; Yu et al., 2016), Na<sup>+</sup> shows weak polarization at the interface of soil colloids and is thus a better choice for determining the effects of soil internal forces on splash erosion. Na<sup>+</sup>-saturated soil samples were used throughout the study. Herein, Na<sup>+</sup>-saturated soil samples were prepared as described in our previous study (Yu et al., 2016). Soil samples of about 1.5 kg were exchanged with Na<sup>+</sup> by adding 0.5 mol L<sup>-1</sup> NaCl solution, and this procedure was repeated for three times. The samples were then washed with deionized water to remove excess Na<sup>+</sup> in the suspension, oven dried at 60 °C, and crushed through a 5 mm sieve to collect model aggregates with diameter of < 5 mm for the experiments.

### 2.3. Experimental method for rainfall splash erosion

The experimental procedures for splash erosion were the same as those in our previous study (Hu et al., 2018). Herein, we briefly introduce the procedures. The devices for splash erosion (shown in Fig. 1) consist of rainfall simulator and splash pan. The rainfall simulator is a cylindrical box with an open top. Syringe needles with a diameter of 0.6 mm were installed uniformly at the bottom of the cylinder. The rainfall intensity was controlled by adjusting the water head through a hole in the cylinder. The splash pan was made up of collecting and test areas. The collecting area was an inclined plane holder with an outlet connected to the lowest point of the plane. Any splashed material was collected from the test area during rainfall simulation. The test area was a circular sieve with a diameter of 10 cm and a height of 1 cm. The mesh size was 0.25 mm to prevent the effect of water film on raindrop impact.

Electrolyte solution and ethanol were employed as rain materials to quantitatively distinguish the contribution of soil internal and external forces to splash erosion. The electrolyte solution as rain material represents the combined effects of soil internal and raindrop impact forces on splash erosion. Thus, we can quantitatively evaluate the combined effects of soil internal and raindrop impact forces on splash

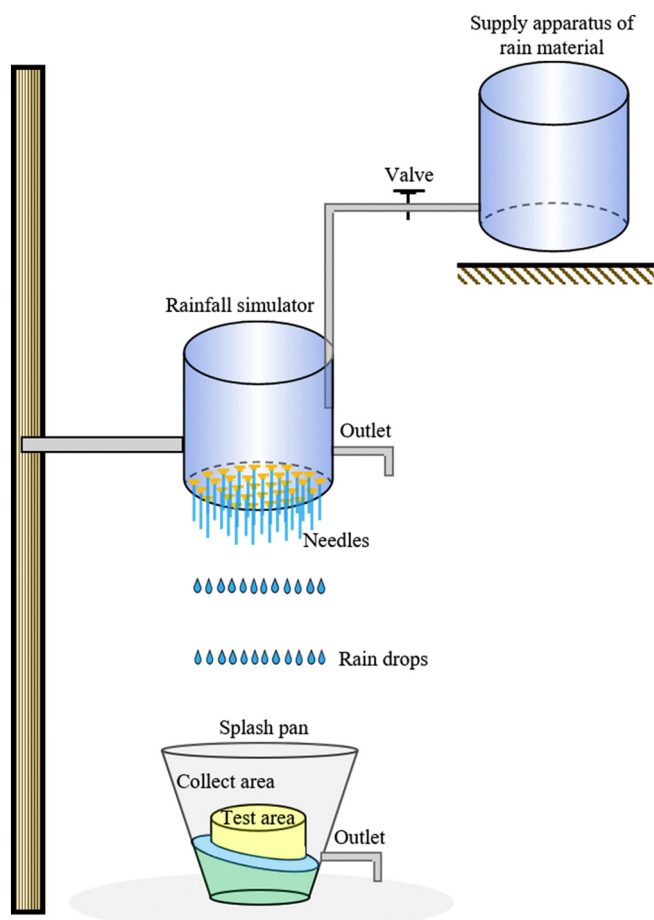


Fig. 1. Schematic drawing of the experiment device.

erosion. Ethanol was used as rain material to simulate the sole effect of raindrop impact force on splash erosion because of the following: first, ethanol could decrease slaking effect and finally protect aggregates from disintegration (Le Bissonnais, 1996). This is possibility due to the weak polarizability of ethanol which could change the surface tension, viscosity, and contact angle, thus finally reduce soil particles interaction forces; second, for ethanol, the smaller dielectric constant (compared with water) could result in the compressed diffuse layer of particles (De Rooy et al., 1980; Permien and Lagaly, 1994; Lagaly and Ziesmer, 2003; Chen et al., 2017) and reduce the electrical repulsion force among the particles (Permien and Lagaly, 1994). Therefore, rainfall with ethanol could maintain the kinetic energy of raindrops, but it did not provide the strong hydration force or other forces that affect the soil structure. Consequently, ethanol could be used to evaluate the sole effect of raindrop impact force on splash erosion.

For splash detachment experiments,  $\text{Na}^+$ -saturated model aggregates ( $< 5 \text{ mm}$ ) were uniformly loaded onto the test area. According to the volume of circular sieve and the total mass of the soil samples, the soil bulk density in splash pan was set as  $1.2 \text{ g cm}^{-3}$  based on the volume of circular sieve and the total mass of soil samples in splash pan. The average rainfall intensity was set as  $60 \text{ mm h}^{-1}$ . To achieve different raindrop kinetic energies, we changed the rainfall height under the same rainfall intensity and raindrop size. The raindrop height was set as 0.4, 0.8, 1.2, 1.6, and 2.0 m. When rainfall began, we collected splashed aggregate fragments at an interval of 30 s. We ended the experiments when a continuous water film appeared on the surface of the splash pan. The total mass of the splashed soil particles was measured, and splash erosion rate was calculated. In this work, splash erosion rate is defined as the total mass of splashed soil particles per unit area per unit time. Two replicates were performed for each run.

## 2.4. Calculations of soil internal forces

The net pressure ( $P_{\text{net}}$ ) of soil internal forces is the sum of electrostatic pressure ( $P_{\text{ele}}$ ), hydration pressure ( $P_{\text{hyd}}$ ), and van der Waals pressure ( $P_{\text{vdw}}$ ). Detailed calculation procedures can be found in our previous work (Hu et al., 2018). Here,  $P_{\text{net}}$  can be calculated using the following equation:

$$P_{\text{net}} = P_{\text{ele}} + P_{\text{hyd}} + P_{\text{vdw}} \quad (1)$$

in which

$$P_{\text{ele}} = \frac{2}{101} RTc_0 \left\{ \cosh \left[ \frac{ZF\phi(d/2)}{RT} \right] - 1 \right\} \quad (2)$$

$$P_{\text{hyd}} = 3.33 \times 10^4 e^{-5.76 \times 10^9 d} \quad (3)$$

$$P_{\text{vdw}} = \frac{A}{0.6\pi} (10d)^{-3} \quad (4)$$

where  $R$  ( $\text{J mol}^{-1} \text{ K}^{-1}$ ) is gas constant,  $T$  (K) is the absolute temperature,  $c_0$  ( $\text{mol L}^{-1}$ ) is the equilibrium concentration of the cation in the bulk solution,  $Z$  is the valence of cation,  $F$  ( $\text{C mol}^{-1}$ ) is Faraday's constant,  $\phi(d/2)$  (V) is the potential at the middle of the overlapping position of the electric double layers of two adjacent particles,  $d$  (dm) is the distance between two adjacent particles, and  $A$  (J) is effective Hamaker constant.

## 2.5. Determination of rainfall kinetic energy

Raindrop diameter is a key parameter used to calculate rainfall kinetic energy. Here, the raindrop shape was assumed as a perfect sphere, and raindrop diameter ( $d$ ) can be calculated as follows:

$$d = \sqrt[3]{\frac{6m}{\pi\rho}} \times 10 \quad (5)$$

where  $m$  (g) is the mass of one raindrop, and  $\rho$  ( $\text{g cm}^{-3}$ ) is the raindrop density (1 and  $0.79 \text{ g cm}^{-3}$  for electrolyte solutions and ethanol, respectively).

Individual raindrop kinetic energy ( $e$ ) can be calculated through the following equation (Hu et al., 2016):

$$e = \frac{1}{2} mv^2 \quad (6)$$

in which

$$v = v_t \sqrt{1 - \exp\left(\frac{-2gh}{v_t^2}\right)} \quad (7)$$

where  $v$  ( $\text{m s}^{-1}$ ) is the velocity of raindrop upon touching the soil surface, and  $v_t$  ( $\text{m s}^{-1}$ ) is the terminal velocities of the raindrops under natural rainfall condition; where  $v_t = (17.20 - 0.844d)\sqrt{0.1d}$ ,  $g$  ( $\text{m s}^{-2}$ ) is the gravitational acceleration, and  $h$  (m) is the rainfall height.

Total rainfall kinetic energy ( $E$ ) can be derived using the following equation:

$$E = \frac{N \times e}{A} \times 10^4 \quad (8)$$

where  $E$  ( $\text{J m}^{-2} \text{ min}^{-1}$ ) is the unit kinetic energy per unit area and time,  $N$  is the number of raindrop in 1 min, and  $A$  ( $\text{m}^2$ ) is the area of the raindrop impact.

Additional details on the calculation of rainfall kinetic energy can be found in the study of Hu et al. (2016).

## 3. Results and discussion

### 3.1. Soil internal and raindrop impact forces

The net pressure produced by soil internal forces could be adjusted

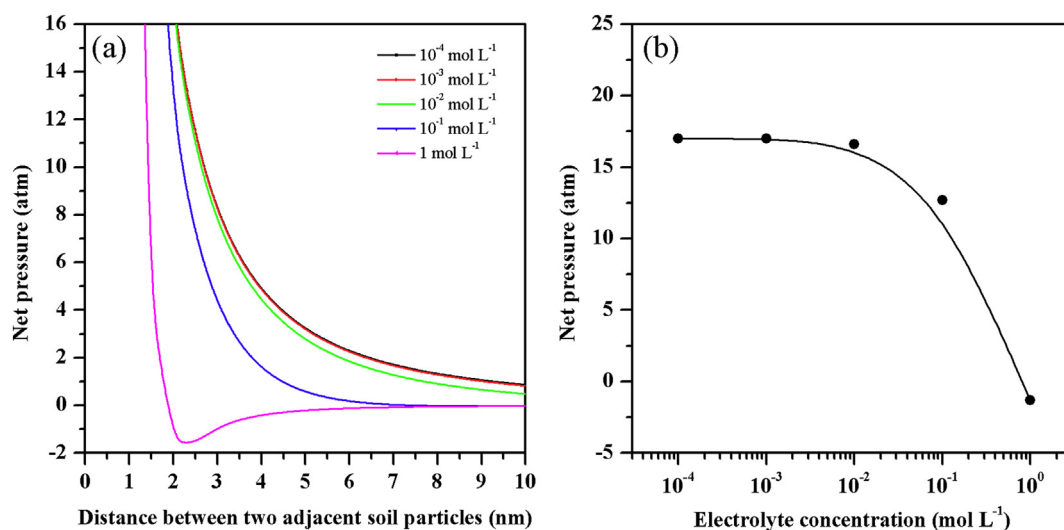


Fig. 2. Net pressure at different distance between two adjacent soil particles (a) and at 2 nm distance between particles under different electrolyte concentration (b).

by changing the electrolyte concentration in the bulk solution. The net pressure between two adjacent soil particles at a given distance and electrolyte concentration can be plotted (Fig. 2). Fig. 2a shows that: (1) the net pressure of soil internal forces could reach as high as hundreds of thousands of atmosphere when two adjacent soil particles infinitely approached in an aqueous system. For example, the net pressure can reach to 1082 and 148 atm at the distance of 0.6 and 1 nm, respectively, between two adjacent soil particles; (2) a strong repulsive pressure at any electrolyte concentration occurs when the distance between two adjacent particles is  $< 1.5$  nm; (3) the changing curves of net pressure almost overlapped when the electrolyte concentration in the bulk solution is  $\leq 10^{-2}$  mol L<sup>-1</sup>, indicating that the net pressure produced by soil internal forces is constant in all circumstances; and (4) net attractive pressure was present at an electrolyte concentration of 1 mol L<sup>-1</sup> at a distance of approximately 2 nm between soil particles.

To further justify the effect of electrolyte concentration on soil internal forces, we directly plotted the net pressure and electrolyte concentration (Fig. 2b). This figure shows the changes in net pressure at a distance of 2 nm between soil particles with electrolyte concentration in the bulk solution. The net pressure first increased as the electrolyte concentration decreased from 1 to  $10^{-2}$  mol L<sup>-1</sup> and then leveled off as the electrolyte concentration decreased from  $10^{-2}$  to  $10^{-4}$  mol L<sup>-1</sup>. The electrolyte concentration of  $10^{-2}$  mol L<sup>-1</sup> is a critical point for splash erosion. When the electrolyte concentration is  $\leq 10^{-2}$  mol L<sup>-1</sup>, the mean value of the net pressure between soil particles reached as high as 16.9 atm. Furthermore, the net pressure at an electrolyte concentration of 1 mol L<sup>-1</sup> was equal to  $-1.3$  atm (Fig. 2b).

The changing trends of net pressure with electrolyte concentration in the bulk solution are in accordance with those previously reported; that is, the net pressure between two adjacent particles could reach hundreds of thousands of atmosphere (Yu et al., 2016). The pressure increases first and then stabilizes with decreasing electrolyte concentrations for soils classified as Calcic Cambisols, Regosols, and Aquic Inceptisols, according to the FAO soil classification (Li et al., 2013; Hu et al., 2015, 2018; Yu et al., 2017). This finding could be mainly attributed to the suppression of the double layer of colloidal particles with increasing electrolyte concentration (Liang et al., 2007). This reaction shows that electrolyte concentration in the bulk solution can greatly affect soil internal forces. Here, it is necessary to point out that the rainwater cannot immediately fill in all the pores within the aggregate at the beginning of rain. However, as long as the rainwater contacts with the particles within the aggregate or wets part of its surface, the repulsive electrostatic force could be generated instantly, which leads to the dispersion of aggregates. Secondly, it indeed takes

rather short time for the rainwater to enter into an aggregate. According to previous studies (Zaher et al., 2005; Hu et al., 2015), soil aggregates could be totally broke down only after 8 s as they were immersed into dilute solution. Thirdly, compared with the raindrop impact force (about 1–3 atm), soil internal forces (i.e., the attractive van der Waals force between soil particles) could reach as high as 100–1000 atm. Clearly, the raindrop impact force itself cannot directly break soil aggregates down. Therefore, it is reasonable to emphasize the role of electrolyte solutions as rainfall material in adjusting the electrostatic forces between particles (Liang et al., 2007; Yu et al., 2016). Moreover, when dry aggregates were wetted during rainfall, the electrolyte concentration of soil bulk solution became diluted. Thus, strong internal repulsive forces in soils will always be present and affect aggregate stability and splash erosion.

Table 1 shows the raindrop characteristics and rainfall kinetic energy under various circumstances. The rainfall kinetic energy increased with increasing rainfall height regardless of the rainfall material used in the study. For example, rainfall kinetic energy at a height of 2 m is 4.1 times higher than that at a height of 0.4 m in the electrolyte system. Compared with that of ethanol, the rainfall kinetic energy of the electrolyte solution was stronger possibly due to the difference in the density and size of raindrop. Overall, the result indicates that the rainfall kinetic energy could be adjusted by the rainfall height, and thus the parameter of rainfall kinetic energy could be employed to reflect different raindrop impact forces (Vaezi et al., 2017; Fernández-Raga et al., 2017).

Table 1

Raindrop characteristics and kinetic energy for the simulated rainfall in this study.

Rain material	Mean diameter (mm)	Height (m)	Velocity (m s <sup>-1</sup> )	Rainfall kinetic energy (J m <sup>-2</sup> min <sup>-1</sup> )
Electrolyte	2.66	0.4	2.71	5.78
		0.8	3.71	10.76
		1.2	4.41	15.54
		1.6	4.94	19.32
		2.0	5.36	23.74
Ethanol	2.06	0.4	2.69	3.82
		0.8	3.66	6.92
		1.2	4.32	9.75
		1.6	4.82	12.17
		2.0	5.2	14.42

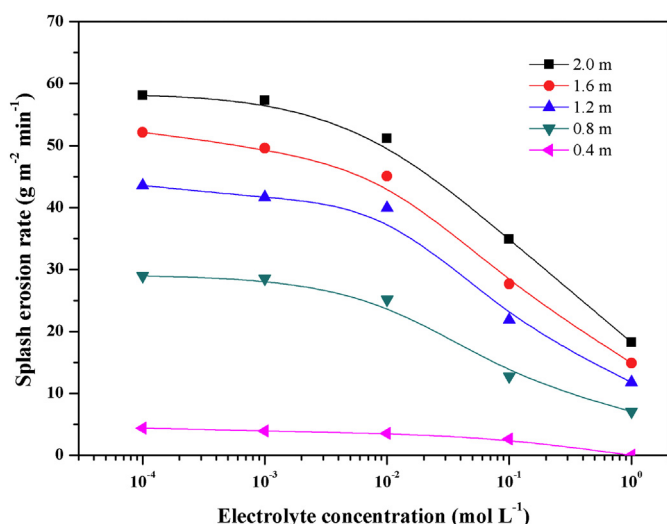


Fig. 3. Changes of soil splash erosion rate with electrolyte concentration at different rainfall heights.

### 3.2. Effects of soil internal forces on splash erosion

The concentration of the electrolyte used as rainfall material could greatly affect the rate of soil splash erosion (Fig. 3), indicating that soil internal forces play a critical role in splash erosion. As shown in Fig. 3, except for rainfall at a height of 0.4 m, the splash erosion rate showed similar changing trends, that is, increased dramatically as the electrolyte concentration decreased from 1 to  $10^{-2}$  mol L<sup>-1</sup> and then became relatively stable when the electrolyte concentration decreased from  $10^{-2}$  to  $10^{-4}$  mol L<sup>-1</sup>. Taking a rainfall height of 1.2 m as an example, the increment of the splash erosion rate from the electrolyte concentration of  $1-10^{-2}$  mol L<sup>-1</sup> was 28.15 g m<sup>-2</sup> min<sup>-1</sup>. Meanwhile, the increment was only 3.63 g m<sup>-2</sup> min<sup>-1</sup> at the electrolyte concentration of  $10^{-2}$  to  $10^{-4}$  mol L<sup>-1</sup>. This difference indicates that the electrolyte concentration of  $10^{-2}$  mol L<sup>-1</sup> is the critical point for splash erosion. The changing trends of splash erosion rate with electrolyte concentration agree well with the results of theoretical prediction in Fig. 2. Hence, soil internal forces could greatly affect rainfall splash erosion. The results are in line with our previous study and confirm that soil internal forces initiate aggregate breakdown and subsequent splash erosion (Hu et al., 2018).

At the rainfall height of 0.4 m, the splash erosion rates were 4.39, 3.92, 3.55, 2.65 min<sup>-1</sup> at electrolyte concentrations of  $10^{-4}$ ,  $10^{-3}$ ,  $10^{-2}$ , and  $10^{-1}$  mol L<sup>-1</sup>, respectively. Soil internal forces exerted minimal influence on splash erosion at a relatively low rainfall height because low rainfall height corresponds to limited raindrop capacity, which did not have sufficient energy to transport soil fragments (Legout et al., 2005b; Fu et al., 2016).

### 3.3. Effect of raindrop impact force on splash erosion

Raindrop impact force affects soil splash erosion during rainfall. In general, raindrop kinetic energy is an important parameter that influences splash erosion. Fig. 4 shows the relationship between soil splash erosion rate and rainfall kinetic energy under various electrolyte concentrations and ethanol. The splash erosion rate increased with increasing rainfall kinetic energy for rain simulated with electrolyte solution and ethanol. Rainfall kinetic energy is a well-known indicator of raindrop impact force (Vaezi et al., 2017; Xiao et al., 2018). The findings reveal that soil external (raindrop impact) force is important for splash erosion.

For the same rainfall kinetic energy, splash erosion rates with electrolyte solution are greater than those with ethanol; but the higher

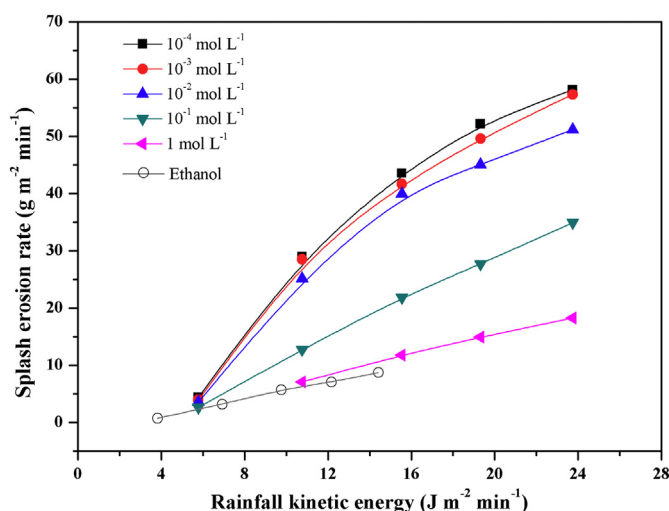


Fig. 4. Changes of soil splash erosion rate with rainfall kinetic energy under various electrolyte concentrations.

the electrolyte concentration, the smaller the difference in splash erosion rates between ethanol and electrolyte solution. The results are similar with previous reports (Xiao et al., 2017, 2018) and could be due to different soil internal forces induced by the electrolyte solution and ethanol in aggregates. In particular, ethanol could influence the surface tension, viscosity, contact angle, and electrostatic repulsion of the interactions between soil and ethanol and these reduce the slaking effect and soil internal forces, and finally increase aggregate stability, and decrease splash erosion (Le Bissonnais, 1996; Barthès and Roose, 2002; Permien and Lagaly, 1994). Therefore, the splash erosion rate when using electrolyte solution should be higher than that with ethanol. On the other hand, with increasing electrolyte concentration of bulk solution, the net pressure between soil particles decreased (Fig. 2b), leading to the decrease in splash erosion rates. Thus, the difference in splash erosion rates between ethanol and electrolyte solution was narrowed down. For the rain simulated with electrolyte solution, the curves of splash erosion rates are close to one another at the electrolyte concentration lower than  $10^{-2}$  mol L<sup>-1</sup>. This result could be explained considering the changes in soil internal forces with electrolyte concentration (Fig. 2).

To quantitatively analyze the relationship between splash erosion rate and rainfall kinetic energy, we fitted the experimental data by applying exponential functions. Table 2 shows the fitted equations between splash erosion rate (*S*) and rainfall kinetic energy (*E*) under various electrolyte solutions and ethanol, respectively. All determination coefficients (*R*<sup>2</sup>) were satisfactory and larger than 0.99.

Table 2

Fitted equations between splash erosion rate (*S*) and rainfall kinetic energy (*E*) under electrolyte solution and ethanol, respectively.

Rain material	Concentration (mol L <sup>-1</sup> )	Fitted equations	<i>R</i> <sup>2</sup>
Electrolyte	$10^{-4}$	$S = -113.2 * \exp.(-E/10.90) + 71.07$	0.9997
	$10^{-3}$	$S = -110.0 * \exp.(-E/11.46) + 71.09$	0.9977
	$10^{-2}$	$S = -101.5 * \exp.(-E/10.15) + 60.83$	0.9975
	$10^{-1}$	$S = -116.9 * \exp.(-E/48.40) + 106.4$	0.9995
	1	$S = -40.32 * \exp.(-E/19.55) + 30.08$	0.9988
Ethanol		$S = -30.30 * \exp.(-E/29.74) + 27.34$	0.9958

**Table 3**  
 Splash erosion rate ( $\text{g m}^{-2} \text{min}^{-1}$ ) under different soil internal and external forces.

$E$	$S_{(I+E)}$					$S_{(E)}$	$S_{(I)}$				
	$10^{-4}$	$10^{-3}$	$10^{-2}$	$10^{-1}$	1		$10^{-4}$	$10^{-3}$	$10^{-2}$	$10^{-1}$	1
$\text{J m}^{-2} \text{min}^{-1}$	$\text{mol L}^{-1}$						$\text{mol L}^{-1}$				
10	25.84	25.13	22.93	11.32	5.90	5.69	20.15	19.43	17.24	5.63	0.21
15	42.48	41.38	37.67	20.65	11.36	9.04	33.44	32.33	28.63	11.61	2.32
20	53.00	51.88	46.68	29.07	15.58	11.87	41.13	40.01	34.81	17.20	3.71
25	59.65	58.67	52.18	36.66	18.86	14.27	45.38	44.40	37.91	22.39	4.59
30	63.85	63.06	55.55	43.50	21.39	16.29	47.56	46.77	39.26	27.21	5.10
35	66.51	65.90	57.60	49.68	23.35	18.00	48.51	47.90	39.60	31.68	5.35
40	68.19	67.74	58.86	55.24	24.87	19.45	48.74	48.29	39.41	35.80	5.42

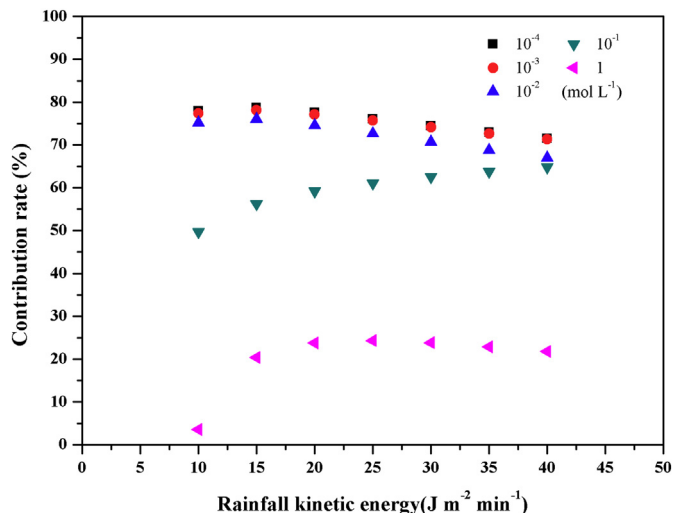


**Fig. 5.** Contribution rates of soil internal forces on splash erosion rate at different rainfall kinetic energy.

**3.4. Contribution rates of soil internal forces on splash erosion**

To assess the contribution of soil internal forces to splash erosion rate, we determined their sole effect first. Based on the fitted equations listed in Table 2, the rates of splash erosion under different soil internal and external forces could be quantitatively estimated (Table 3). In this work, electrolyte solution was used as rain material to reflect the combined effects of soil internal and external forces (raindrop impact force) on splash erosion ( $S_{(I+E)}$ ). Ethanol was also used to represent the sole effect of soil external force (raindrop impact force) on splash erosion ( $S_{(E)}$ ). Thus, the sole effect of soil internal forces on splash erosion ( $S_{(I)}$ ) could be derived from the difference between  $S_{(I+E)}$  and  $S_{(E)}$ .

As shown in Table 3, the soil splash erosion rate increased with increasing rainfall kinetic energy. This result is in line with previous findings, which also reported that the soil splash erosion rate increased with the increase of rainfall kinetic energy (Fu et al., 2016; Vaezi et al., 2017; Xiao et al., 2018). This is mainly due to the fact that strong rainfall kinetic energy means strong ability of transporting fine soil particles. On the other hand, the soil splash erosion rates increased with decreasing electrolyte concentration (Table 3). This result is consistent with previous findings (Kim and Miller, 1996; Haraguchi and Nakaishi, 2008). With decreasing electrolyte concentration of soil bulk solution, the repulsive soil internal forces between soil particles increased (Fig. 2), which could make soil aggregates disintegrate and release large amounts of fine soil particles for splash erosion (Xu et al., 2015). This indicates that the repulsive soil internal forces greatly affect the splash erosion. In addition, the viscosity of raindrops could be changed due to various electrolyte concentrations, which would further affect splash erosion. According to the previous study (Goncalves and Kestin, 1977),

the viscosity was about 0.89 and 0.90 cP at the electrolyte concentrations of  $10^{-4}$  and  $10^{-1}$  mol L<sup>-1</sup> in NaCl solution, respectively. It is clear that the difference in viscosity under those electrolyte concentrations is very small. However, under those circumstances, the surface potentials of soil particles are -350 and -175 mV, respectively, which means the repulsive electrostatic force between soil particles highly differ from each other. Correspondingly, the splash erosion rate showed big difference, e.g., 43.5 and 21.9 g min<sup>-1</sup> m<sup>-2</sup> at the rain height of 1.2 m. This indicates that the differences in splash erosion under different electrolyte concentrations could result from the repulsive interaction forces between soil particles instead of the differences in viscosity. Besides, Yu et al. (2016) also reported that surface tension coefficients of electrolyte concentrations changed slightly from 1 to  $10^{-5}$  mol L<sup>-1</sup>, which thus would have minor effect on soil aggregate stability and water movement. Changes in electrolyte concentration of bulk solution could mainly affect particle interaction forces, which further determined aggregate stability, soil erosion and soil water movement (Kim and Miller, 1996; Liang et al., 2007; Li et al., 2013; Yu et al., 2016). Overall, soil splash erosion depends not only on soil external force (raindrop impact) but also on soil internal forces.

To further quantitatively confirm the important role of soil internal forces on splash erosion, we estimated the contribution rates of soil internal forces on splash erosion rate (CR) at different rainfall kinetic energies. Here, CR was defined as the ratio of  $S_{(I)}$  to  $S_{(I+E)}$ . As shown in Fig. 5, when the electrolyte concentration is  $\leq 10^{-2}$  mol L<sup>-1</sup>, the changes in CR showed similar trend, that is, decreasing with increasing rainfall kinetic energy. In addition, the CR reached > 65%. However, when the electrolyte concentration was higher than  $10^{-2}$  mol L<sup>-1</sup>, the CR showed different changing patterns. To be specific, at the electrolyte concentration of  $10^{-1}$  mol L<sup>-1</sup>, the CR increased with increasing rainfall kinetic energy and was between 50% and 65%. Correspondingly, at the electrolyte concentration of 1 mol L<sup>-1</sup>, the CR first increased and then remained relatively stable with increasing rainfall kinetic energy and was between 3% and 25%. Hence, soil internal forces play a key role in splash erosion when the electrolyte concentration of the soil bulk solution was  $\leq 10^{-1}$  mol L<sup>-1</sup>. In contrast, raindrop impact force has more effect on splash erosion at an electrolyte concentration of 1 mol L<sup>-1</sup>.

These results could be rationalized by experiments on aggregate stability under different electrolyte concentrations in our previous work (Hu et al., 2018). At the electrolyte concentration of  $< 10^{-1}$  mol L<sup>-1</sup>, the aggregate breakdown under strong soil internal forces could provide certain amounts of fine particles for splash erosion. Meanwhile, soil internal forces dramatically decreased at the electrolyte concentration of 1 mol L<sup>-1</sup>, leading to less finer particles ( $< 20 \mu\text{m}$ ) produced for splash detachment. With the increase of electrolyte concentration in bulk solution, soil internal forces decreased, and then soil aggregate stability increased, finally soil erosion rate decreased and soil water infiltration rate increased (Li et al., 2013; Yu et al., 2016). The splash parameters were significantly correlated to soil aggregate stability (Barthès and Roose, 2002). It is indicated that soil internal forces

could affect splash erosion by influencing aggregate stability (Hu et al., 2015). Thus, CRs differ under various soil internal forces.

The electrolyte concentration of soil solution is usually at a magnitude of approximately  $10^{-3}$  mol L<sup>-1</sup> for a natural field soil (Li and Li, 1998). Here, even if we suppose that the rainfall kinetic energy is 60 J m<sup>-2</sup> min<sup>-1</sup>, the CR could be higher than 60%. However, if the electrolyte concentration of the soil solution is  $> 10^{-1}$  mol L<sup>-1</sup>, e.g., for saline or alkaline soils, then the raindrop impact force could be the main contributor to splash erosion. Therefore, we infer that soil internal forces exhibit higher contribution to splash erosion rate compared with raindrop impact force under most natural conditions. This conclusion is indirectly confirmed by other previous studies (Xiao et al., 2017, 2018). Using deionized water and ethanol as rain materials, Xiao et al. (2017, 2018) investigated the effects of slaking and raindrop impact forces on splash erosion through simulated rainfall; the results showed that the slaking effects exhibited higher contribution to aggregate breakdown and splash erosion than raindrop impact. However, slaking is a physical process where soil aggregates are disintegrated either by compressed air in aggregate or by forces generated by clay swelling during wetting (Chan and Mullins, 1994; Zaher and Caron, 2008; Wuddivira et al., 2009). Note that the air pressure in the aggregates during wetting was  $< 1$  atm (Vachaud et al., 1973; Zaher et al., 2005), while soil internal forces could usually be 100–1000 atm. Besides, clay swelling during wetting resulted from surface hydration and an overlap of diffused double layers (Abu-Sharar et al., 1987). Diné and Gregorich (1995) claimed that clay swelling affect soil aggregates more greatly than alterations caused by compressed air during rapid wetting. Together, these studies indicate that the slaking effect could essentially stem from soil internal forces between particles, especially electrostatic and hydration repulsive forces (Levy et al., 2003; Abu-Sharar et al., 1987). Therefore, it is the soil internal forces, not the slaking effect, that initiate the aggregate breakdown and subsequent splash erosion. Soil internal forces have higher contribution to splash erosion rate than raindrop impact force. However, air pressure as a result of the slaking effect is also an important factor that induces soil aggregate breakdown, leading to the release of microaggregates (Le Bissonnais, 1996; Lado et al., 2004; Vermang et al., 2009; Fajardo et al., 2016). Unfortunately, we cannot quantitatively isolate the slaking effect in the present study. The slaking mechanism (air pressure) would intertwine with soil internal forces, which is also a challenging problem (Levy et al., 2003; Haraguchi and Nakaishi, 2008). Notwithstanding its limitation, this study does suggest that repulsive soil internal forces contributed more than raindrop impact force to rainfall splash erosion.

In summary, for the parameter of splash erosion rate (representing the final result of splash erosion), soil internal forces elicited higher contribution to splash erosion during rainfall than raindrop impact force. However, for the entire process of rainfall splash erosion, both repulsive soil internal and raindrop impact forces are critical erosive factors. This result is also in accordance with the philosophical view, the occurrences or events are due to both internal and external causes, and the former is quite important.

#### 4. Conclusions

In this study, electrolyte solution and ethanol were used as rain materials to separate the effects of soil internal and external forces on splash erosion. The splash erosion rate increased with increasing rainfall kinetic energy and net pressure of soil internal forces. For rain using electrolyte concentration, the splash erosion rate increased first (from 1 to  $10^{-2}$  mol L<sup>-1</sup>) then remained stable (from  $10^{-2}$  to  $10^{-4}$  mol L<sup>-1</sup>) with decreasing electrolyte concentration in the bulk solution. The results are in agreement with the theoretical analysis of soil internal forces. In general, the contribution rate of soil internal forces on splash erosion at a low electrolyte concentration ( $< 10^{-2}$  mol L<sup>-1</sup>) is  $> 65\%$ . Overall, soil internal forces could contribute higher to splash erosion under natural conditions than raindrop impact force. For the entire

process of splash erosion, however, the repulsive soil internal and external forces are both important. Our results shed new light on the mechanism of splash erosion and open the possibility of developing methods for controlling soil erosion risk by jointly adjusting the soil internal and external forces.

#### Acknowledgements

This work was supported by the National Natural Science Foundation of China (41601236, 41701261 and 41761144060), the National Key R&D Program of China (2016YFE0202900), the CAS “Light of West China” Program (XAB2016B07), and the Doctoral Start-Up Research Fund of Northwest A&F University (2452016152). The authors are grateful to Dr. Hai Xiao for his helpful suggestions for rainfall simulation experiments in this study.

#### References

- Abu-Sharar, T.M., Bingham, F.T., Rhoades, J.D., 1987. Stability of soil aggregates as affected by electrolyte concentration and composition. *Soil Sci. Soc. Am. J.* 51 (2), 309–314.
- Angulo-Martínez, M., Begueria, S., Navas, A., Machín, J., 2012. Splash erosion under natural rainfall on three soil types in NE Spain. *Geomorphology* 175, 38–44.
- Barthès, B., Roose, E., 2002. Aggregate stability as an indicator of soil susceptibility to runoff and erosion: validation at several levels. *Catena* 47 (2), 133–149.
- Chan, K.Y., Mullins, C.E., 1994. Slaking characteristics of some Australian and British soils. *Eur. J. Soil Sci.* 45 (3), 273–283.
- Chen, T., Zhao, Y., Song, S., 2017. Comparison of colloidal stability of montmorillonite dispersion in aqueous NaCl solution with in alcohol-water mixture. *Powder Technol.* 322, 378–385.
- De Rooy, N., De Bruyn, P.L., Overbeek, J.T.G., 1980. Stability of dispersions in polar organic media. I. Electrostatic stabilization. *J. Colloid Interface Sci.* 75 (2), 542–554.
- Diné, H., Gregorich, E., 1995. Structural stability status as affected by long-term continuous maize and bluegrass sod treatments. *Biol. Agric. Hortic.* 12 (3), 237–252.
- Fajardo, M., Mcbratney, A.B., Field, D.J., Minasny, B., 2016. Soil slaking assessment using image recognition. *Soil Tillage Res.* 163, 119–129.
- Falsone, G., Bonifacio, E., Zanini, E., 2012. Structure development in aggregates of poorly developed soils through the analysis of the pore system. *Catena* 95, 169–176.
- Fernández-Raga, M., Fraile, R., Keizer, J.J., Teijeiro, M.E.V., Castro, A., Palencia, C., Calvo, A.L., Koenders, J., Marques, R.L.D., 2010. The kinetic energy of rain measured with an optical disdrometer: an application to splash erosion. *Atmos. Res.* 96, 225–240.
- Fernández-Raga, M., Palencia, C., Keesstra, S., Jordán, A., 2017. Splash erosion: a review with unanswered questions. *Earth Sci. Rev.* 171, 463–477.
- Fu, Y., Li, G., Zheng, T., Li, B., Zhang, T., 2016. Impact of raindrop characteristics on the selective detachment and transport of aggregate fragments in the Loess Plateau of China. *Soil Sci. Soc. Am. J.* 80 (4), 1071–1077.
- Goncalves, F.A., Kestin, J., 1977. The viscosity of NaCl and KCl solutions in the range 25–50 °C. *Ber. Bunsenges. Phys. Chem.* 81 (11), 1156–1161.
- Haraguchi, N., Nakaishi, K., 2008. Breakdown process of aggregates with non-swelling and swelling clays as affected by electrolyte concentration and air condition. *Clay Sci.* 14 (1), 33–42.
- Holthausen, D., Peth, S., Horn, R., 2010. Impact of potassium concentration and matric potential on soil stability derived from rheological parameters. *Soil Till. Res.* 111, 75–85.
- Hu, F.N., Xu, C.Y., Li, H., Li, S., Yu, Z., Li, Y., He, X.H., 2015. Particles interaction forces and their effects on soil aggregates breakdown. *Soil Tillage Res.* 147, 1–9.
- Hu, W., Zheng, F., Bian, F., 2016. The directional components of splash erosion at different raindrop kinetic energy in the Chinese Mollisol region. *Soil Sci. Soc. Am. J.* 80 (5), 1329–1340.
- Hu, F.N., Liu, J.F., Xu, C.Y., Wang, Z.L., Liu, G., Li, H., Zhao, S.W., 2018. Soil internal forces initiate aggregate breakdown and splash erosion. *Geoderma* 320, 43–51.
- Huang, X.R., Li, H., Li, S., Xiong, H.L., Jiang, X.J., 2016. Role of cationic polarization in humus-increased soil aggregate stability. *Eur. J. Soil Sci.* 67 (3), 341–350.
- Jayawardena, A.W., Rezaur, R.B., 2000. Drop size distribution and kinetic energy load of rainstorms in Hong Kong. *Hydrol. Process.* 14 (6), 1069–1082.
- Kim, K.H., Miller, W.P., 1996. Effect of rainfall electrolyte concentration and slope on infiltration and erosion. *Soil Technol.* 9 (3), 173–185.
- Kinnell, P.I.A., 2005. Raindrop-impact-induced erosion processes and prediction: a review. *Hydrol. Process.* 19 (14), 2815–2844.
- Lado, M., Ben-Hur, M., Shainberg, I., 2004. Soil wetting and texture effects on aggregate stability, seal formation, and erosion. *Soil Sci. Soc. Am. J.* 68, 1992–1999.
- Lagaly, G., Ziesler, S., 2003. Colloid chemistry of clay minerals: the coagulation of montmorillonite dispersions. *Adv. Colloid Interf. Sci.* 100, 105–128.
- Le Bissonnais, Y., 1996. Aggregate stability and assessment of soil crustability and erodibility: I. Theory and methodology. *Eur. J. Soil Sci.* 47 (4), 425–437.
- Le Bissonnais, Y., Singer, M.J., 1993. Seal formation, runoff and interrill erosion from seventeen California soils. *Soil Sci. Soc. Am. J.* 57, 224–229.
- Legout, C., Lagueolis, S., Le Bissonnais, Y., 2005a. Aggregate breakdown dynamics under rainfall compared with aggregate stability measurements. *Eur. J. Soil Sci.* 56 (2),

- 225–238.
- Legout, C., Leguedois, S., Le Bissonnais, Y., Malam Issa, O., 2005b. Splash distance and size distributions for various soils. *Geoderma* 124 (3), 279–292.
- Levy, G.J., Mamedov, A.I., Goldstein, D., 2003. Sodicity and water quality effects on slaking of aggregates from semi-arid soils. *Soil Sci.* 168 (8), 552–562.
- Li, Y.Z., Li, B.G., 1998. *Soil Solute Transport*. Science Press, Beijing.
- Li, H., Hou, J., Liu, X.M., Li, R., Zhu, H., Wu, L.S., 2011. Combined determination of specific surface area and surface charge properties of charged particles from a single experiment. *Soil Sci. Soc. Am. J.* 75 (6), 2128–2135.
- Li, S., Li, H., Xu, C.Y., Huang, X.Y., Xie, D.T., Ni, J.P., 2013. Particle interaction forces induce soil particle transport during rainfall. *Soil Sci. Soc. Am. J.* 77 (5), 1563–1571.
- Li, S., Li, H., Hu, F.N., Huang, X.Y., Xie, D.T., Ni, J.P., 2015. Effects of strong ionic polarization in the soil electric field on soil particle transport during rainfall. *Eur. J. Soil Sci.* 66 (5), 921–929.
- Liang, Y., Hilal, N., Langston, P., Starov, V., 2007. Interaction forces between colloidal particles in liquid: theory and experiment. *Adv. Colloid Interf. Sci.* 134, 151–166.
- Lu, J.Y., Su, C.C., Lu, T.F., Maa, M.M., 2008. Number and volume raindrop size distributions in Taiwan. *Hydrol. Process.* 22, 2148–2158.
- Ma, R.M., Li, Z.X., Cai, C.F., Wang, J.G., 2014. The dynamic response of splash erosion to aggregate mechanical breakdown through rainfall simulation events in Ultisols (subtropical China). *Catena* 121, 279–287.
- Mekonnen, M., Keesstra, S., Stroosnijder, L., Baartman, J., Maroulis, J., 2015. Soil conservation through sediment trapping: a review. *Land Degrad. Dev.* 26, 544–556.
- Oliveira, P.T.S., Wendland, E., Nearing, M.A., 2013. Rainfall erosivity in Brazil: a review. *Catena* 100, 139–147.
- Parras-Alcántara, L., Lozano-García, B., Keesstra, S., Cerdà, A., Brevik, E.C., 2016. Long-term effects of soil management on ecosystem services and soil loss estimation in olive grove top soils. *Sci. Total Environ.* 571, 498–506.
- Pieri, L., Bittelli, M., Hanuskova, M., Ventura, F., Vicari, A., Pisa, P.R., 2009. Characteristics of eroded sediments from soil under wheat and maize in the North Italian Apennines. *Geoderma* 154 (1), 20–29.
- Permien, T., Lagaly, G., 1994. The rheological and colloidal properties of bentonite dispersions in the presence of organic compounds III. The effect of alcohols on the coagulation of sodium montmorillonite. *Colloid Polym. Sci.* 272 (10), 1306–1312.
- Shainberg, I., Levy, G.J., Rengasamy, P., Frenkel, H., 1992. Aggregate stability and seal formation as affected by drops' impact energy and soil amendments. *Soil Sci.* 154 (2), 113–119.
- Sparks, D.L., Page, A.L., Helmke, P.A., Loeppert, R.H., Soltanpour, P.N., Johnston, C.T., Sumner, M.E., 1996. *Methods of Soil Analysis Part 3: Chemical Methods*. Soil Science Society of America Inc., Madison, WI.
- Uri, N.D., 2000. Conservation practices in us agriculture and their implication for global climate change. *Sci. Total Environ.* 256, 23–38.
- Vachaud, G., Vauclin, M., Khanji, D., Wakil, M., 1973. Effects of air pressure on water flow in an unsaturated stratified vertical column of sand. *Water Resour. Res.* 9 (1), 160–173.
- Vaezi, A.R., Bahrami, H.A., 2014. Relationship between soil productivity and erodibility in rainfed wheat lands in northwestern Iran. *J. Agric. Sci. Technol.* 16, 1455–1466.
- Vaezi, A.R., Ahmadi, M., Cerdà, A., 2017. Contribution of raindrop impact to the change of soil physical properties and water erosion under semi-arid rainfalls. *Sci. Total Environ.* 583, 382–392.
- Vermang, J., Demeyer, V., Cornelis, W.M., Gabriels, D., 2009. Aggregate stability and erosion response to antecedent water content of a loess soil. *Soil Sci. Soc. Am. J.* 73 (3), 718–726.
- Warrington, D.N., Mamedov, A.I., Bhardwaj, A.K., Levy, G.J., 2009. Primary particle size distribution of eroded material affected by degree of aggregate slaking and seal development. *Eur. J. Soil Sci.* 60 (1), 84–93.
- Wei, W., Chen, L., Fu, B., Huang, Z., Wu, D., Gui, L., 2007. The effect of land uses and rainfall regimes on runoff and soil erosion in the semi-arid loess hilly area, China. *J. Hydrol.* 335 (3), 247–258.
- Wuddivira, M.N., Stone, R.J., Ekwue, E.I., 2009. Clay, organic matter, and wetting effects on splash detachment and aggregate breakdown under intense rainfall. *Soil Sci. Soc. Am. J.* 73, 226–232.
- Xiao, H., Liu, G., Abd-Elbasit, M.A.M., Zhang, X.C., Liu, P.L., Zheng, F.L., Zhang, J.Q., Hu, F.N., 2017. Effects of slaking and mechanical breakdown on disaggregation and splash erosion. *Eur. J. Soil Sci.* 68 (6), 797–805.
- Xiao, H., Liu, G., Zhang, Q., Zheng, F., Zhang, X., Liu, P., Zhang, J., Hu, F., Abd-Elbasit, M.A.M., 2018. Quantifying contributions of slaking and mechanical breakdown of soil aggregates to splash erosion for different soils from the Loess plateau of China. *Soil Tillage Res.* 178, 150–158.
- Xu, C.Y., Li, H., Hu, F.N., Li, S., Liu, X.M., Li, Y., 2015. Non-classical polarization of cations increases the stability of clay aggregates: specific ion effects on the stability of aggregates. *Eur. J. Soil Sci.* 66 (3), 615–623.
- Yaghobi, A., Khalilimoghadam, B., Saedi, T., Rahnama, M., 2018. The effect of enclosure management on the reduction of SOC loss due to splash erosion in gypsiferous soils in southwestern Iran. *Geoderma* 319, 34–42.
- Yu, Z.H., Liu, X.M., Xu, C.Y., Xiong, X.L., Li, Hang, 2016. Specific ion effects on soil water movement. *Soil Tillage Res.* 161, 63–70.
- Yu, Z., Zhang, J., Zhang, C., Xin, X., Li, H., 2017. The coupling effects of soil organic matter and particle interaction forces on soil aggregate stability. *Soil Tillage Res.* 174, 251–260.
- Zaher, H., Caron, J., 2008. Aggregate slaking during rapid wetting: hydrophobicity and pore occlusion. *Can. J. Soil Sci.* 88 (1), 85–97.
- Zaher, H., Caron, J., Ouaki, B., 2005. Modeling aggregate internal pressure evolution following immersion to quantify mechanisms of structural stability. *Soil Sci. Soc. Am. J.* 69 (1), 1–12.
- Zhang, S., Fan, W., Li, Y., Yi, Y., 2017. The influence of changes in land use and landscape patterns on soil erosion in a watershed. *Sci. Total Environ.* 574, 34–45.
- Ziadat, F.M., Taimeh, A.Y., 2013. Effect of rainfall intensity, slope, land use and antecedent soil moisture on soil erosion in an arid environment. *Land Degrad. Dev.* 24 (6), 582–590.